RESEARCH ARTICLE doi.org/10.1002/adsc.202300819 Advanced Synthesis & Catalysis

Integrating Chemocatalysis and Enzyme Engineering for Coproduction of Bioplastic Precursors Butanediol and Succinic Acid from Xylose

Samuel Sutiono,[a, b, e] Okke Melse,[a, b, f] Manuel Döring,[a, b] Petra Lommes,[a] and Volker Sieber[a, b, c, d,*]

[a] Chair of Chemistry of Biogenic Resources, Campus Straubing for Biotechnology and Sustainability, Technical University of Munich, 94315 Straubing, Germany
E-mail: sieber@tum.de
[b] SynBioFoundry@TUM, Technical University of Munich, Schulgasse 22, 94315 Straubing, Germany
[c] Catalytic Research Center, Technical University of Munich, Ernst-Otto-Fischer-Straße 1, 85748 Garching, Germany
[d] School of Chemistry and Molecular Biosciences, The University of Queensland, 68 Copper Road, St. Lucia 4072, Australia
[e] Present address: CarboCode GmbH, Byk-Gulden-Straße 2, 78467 Konstanz, Germany
[f] Present address: Biozentrum University of Basel, Spitalstrasse 41, 4056 Basel, Switzerland

Manuscript received: July 31, 2023; Revised manuscript received: November 28, 2023;
Version of record online: December 14, 2023

Supporting information for this article is available on the WWW under https://doi.org/10.1002/adsc.202300819

Abstract: Polybutylene succinate (PBS) is one of the most important biobased plastics, based on the amount produced. Owing to its high melting point and resemblance to petroleum-based plastics (i. e. PP), PBS becomes one of the emerging bioplastics with an array of applications. PBS is manufactured by polymerization of 1,4-butanediol and succinic acid. Thus, it is of great importance to ensure the use of renewable resources to produce the PBS precursors. As the second most abundant carbohydrate monomer on Earth, D-xylose will be a suitable candidate for this purpose. In this work, we combined protein engineering with chemical oxidation by gold catalyst to enable transformation of D-xylose to 1,4-butanediol and succinic acid simultaneously. *In silico* docking studies and semi rational design were employed to create variants of the key enzyme, branched chain α-keto acid decarboxylase (KdcA) with higher affinity for the intermediates in the production of 1,4-butanediol and succinic acid. Direct enzymatic biotransformation would result in a production of both monomers with 3:1 ratio, thus not readily suitable for a direct polymerization to PBS. By developing a one-pot multi-step chemo-enzymatic approach with a gold catalyst to perform the first oxidation step, we could achieve a final product ratio of 1:1. Application of an engineered KdcA variant allowed us to achieve >98% yield after four hours transformation. In contrast, after 24 h transformation, >10% intermediate was still observed when the original variant was used. We anticipate this new approach could serve as an alternative route for biotechnological productions of PBS and its precursors.

Keywords: Bioplastics; 1,4-butanediol; succinic acid; biomass; protein engineering; chemo-enzymatic; biocatalysis; gold catalyst

Introduction

In the past years, utilization of second-generation biomass for chemicals production has attracted much attention as it is not directly competing with food application. Waste biomass is usually made of lignocellulose of which hemicellulose is a major component. As a major constituent of hemicellulose, D-xylose is the second most abundant monomer on Earth after D-glucose. Thus, development of D-xylose-based

biotransformations is of great importance.[1–3] Many chemicals have been derived from D-xylose, in particular by modifying the ATP-independent microbial pathways (Dahm and Weimberg pathways), by introducing synthetic pathways to microorganisms or by developing enzymatic based biotransformations. Generally, the modification relies either on an aldolase that splits the D-xylose derivative to pyruvate and glycolaldehyde or on a decarboxylase that acts on α-keto acid derivatives of D-xylose.[2,4,5]

The first pathway is typically used to make C2-3 chemicals, such as ethanol and lactic acid (derived from pyruvate) as well as glycolic acid and ethylene glycol (derived from glycolaldehyde). On the other hand, the second pathway is utilized to make C4-5 chemicals, such as 1,2,4-butanetriol (BTO), 3-hydroxy-γ-butyrolactone (HBL), and 1,4-butanediol (BDO). The aldolase-based pathway has an advantage for direct compatibility with synthetic pathways from biomass-derived D-glucose as they share pyruvate as a central intermediate. On the other hand, the decarboxylase-based pathway has an advantage of higher atom economy and the C4-5 chemicals derived from the decarboxylase-pathway are typically not readily accessible from D-glucose, i.e. requiring significantly longer pathways than of D-xylose.[2,4,5]

There are several decarboxylases that have been applied in the decarboxylase-based pathway, but the most notable enzyme is the branched chain keto acid decarboxylase from *Lactococcus lactis* (*Ll*KDC). There are two isoenzymes of KDC, namely KdcA and KivD. Both have similar activity and substrate profile.[6,7] Many engineering efforts have been implemented on KivD but with the strong focus on the production of primary longer chain alcohols, such as isobutanol, 1-pentanol or 1-octanol.[8,9] The key enzyme controlling the production of BTO, HBL and BDO is KDC. It acts as a gate keeper, whose activity towards three possible intermediates has a major influence on the type of product being formed (Scheme 1). Accordingly, it is of interest to increase the activity and expand the substrate profile of KDC to achieve formation of the desired product. In particular, decarboxylation of α-ketoglutarate (aKG) by KDC has never been reported in literature. So far, this activity has been only reported from a highly specific aKG decarboxylases, which plays a role in a variant of the TCA cycles.[10] This new activity of KDC will give access to succinic acid from D-xylose, another important building block next to BTO, HBL, and BDO.

Succinic acid and BDO have jointly been applied as the building block for polybutylene succinate (PBS), an emerging bioplastic. PBS is a highly crystalline polyester with physical properties similar to that of polypropylene (PP) and the crystallization behavior similar to that of polyethylene (PE). Furthermore, the biodegradability and the thermoplasticity of PBS make it attractive for a wide range of applications. Hitherto, the monomer constituents of PBS are still traditionally produced from petrochemicals, depreciating the "bio" status of PBS.[11,12] With the growth projection of bioplastics production to reach 5.3 million ton in 2026, 16% of which comprises PBS, it becomes attractive to diversify the source of renewable materials for bio-based succinic acid and BDO production.[13]

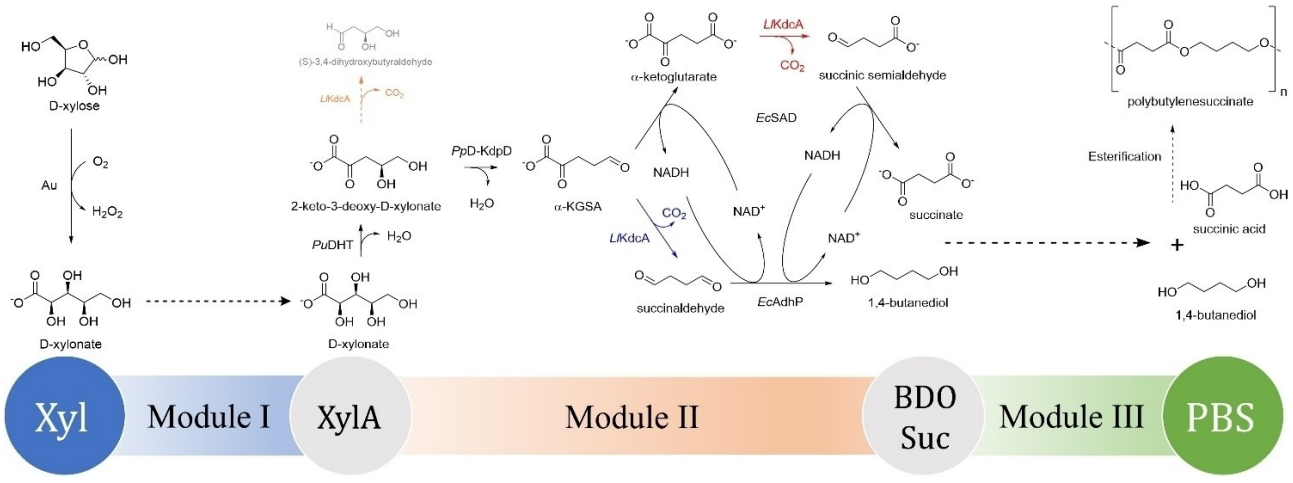

Scheme 1. Chemo-enzymatic transformation of D-xylose to polybutylene succinate (PBS) consisting of three modules. Module I is chemical oxidation of D-xylose to D-xylonate. Module II is cell-free biotransformation of D-xylonate to 1,4-butanediol and succinic acid. Module III is esterification of 1,4-butanediol and succinic acid to polybutylene succinate. This work focuses on the development of Module I and II. Side reactivity of KdcA can potentially lead to the formation of the undesired byproduct, (S)-3,4-dihydroxybutyraldehyde (labelled gray). Organic acids in Modules I and II are depicted as deprotonated because the reaction was performed at pH ≥ 7.

In previous studies, KdcA has been shown as promising enzyme to perform decarboxylation of α-ketoglutarate semialdehyde (KGSA) (k_{cat}/K_M: 2.2 s^{-1} mM^{-1}), the precursor of BDO.[14,15] In this work, we aimed to tailor KdcA further to accept aKG (k_{cat}/K_M: < 0.1 s^{-1} mM^{-1}). We combined semi-rational design and molecular dynamics analysis to create suitable variants to perform decarboxylation not only of aKG but also of KGSA. The increased promiscuity feature of our variants would make it possible to coproduce succinic acid and BDO from D-xylose. Accordingly, we designed a cell-free enzymatic biomanufacturing process in combination with a chemical catalyst to enable cofactor-balanced *in vitro* biotransformation of D-xylose into equal amounts of succinic acid and BDO (Scheme 1).

Results and Discussion

In silico Identification of Mutation Libraries

An initial activity test suggests that KdcA only possesses negligible activity toward aKG (Var. 1, Table 1), illustrating the necessity to engineer this enzyme to have better proficiency toward aKG, while still maintaining or improving activity toward KGSA. Here, we combined *in silico* studies with iterative semi rational design to reach this goal.

For *in silico* docking studies we used the crystal structures of KdcA, which has been solved at 1.80 Å resolution (PDB-ID: 2vbg).[16] In both structures, the loops at position 182–187 and 342–344 are missing. We resolved the loops by replacing them in 2vbg with the loops from a structure predicted by AlphaFold.[17] Afterwards, we defined the most-likely protonation state of the binding site residues by analyzing important hydrogen-bond networks, and docked both KGSA and aKG in KdcA using AutoDock VINA. We observed that for the majority of the poses, including the highest-scored ones, the substrate forms hydrogen bonds with S286, Q377, E462, and H112. We further refined the poses by 200 ns molecular dynamics simulations in wild type KdcA, in which we observed a highly stable KGSA binding, while aKG was much more flexible and could adopt multiple binding poses, which might explain the lower catalytic efficiency towards aKG. Additional molecular dynamics simulations starting from alternative docked poses were also performed, but these simulations showed a highly unstable substrate binding, occasionally ending up in binding orientations similar to the top-ranked poses.

From these *in silico* studies the amino acids were revealed that shape the substrate binding pocket of KdcA (Figure 1 A and B). We then decided to do the first round of screening by building libraries targeting individual amino acids shaping the binding pocket at positions 286, 377, 381, 382, 461, 465, 538, and 542. Additionally, we also included amino acids at position 402. A previous study shows that mutating this position was beneficial for substrates with longer chains.[9] Thus, we also included this position in our first screening campaign. In the first round of semi-

Table 1. Kinetics parameter of KdcA variants determined by coupled assay. The reaction was performed in 50 mM KPi buffer pH 7.0 containing $MgCl_2$ 2.5 mM and ThDP 0.1 mM at 30 °C.[a]

Var.	Substitutions	KGSA				aKG[b]			T_m (°C)
		k_{cat} (s^{-1})	K_M (mM)	Ki (mM)	k_{cat}/K_M (s^{-1} mM^{-1})	k_{cat} (s^{-1})	K_M (mM)	k_{cat}/K_M (s^{-1} mM^{-1})	
1[c]	Q252N/D306G/E316R/F388Y	2.6 ± 0.1	1.2 ± 0.1	79.6 ± 9.9	2.15	(0.6 ± 0.0)	n.d.	55.4×10^{-3}	63.5
2	S286T	3.9 ± 0.1	1.0 ± 0.1	85.4 ± 10.9	3.62	(0.7 ± 0.0)	n.d.	73.4×10^{-3}	69.5
3	Q377T	4 ± 0.1	0.5 ± 0.0	113.5 ± 15.0	8.61	(4.1 ± 0.0)	n.d.	405×10^{-3}	60.5
4	Q377I	3.2 ± 0.1	0.4 ± 0.0	190.5 ± 8.1	7.57	0.2 ± 0.0	39.3 ± 4.6	5.1×10^{-3}	61.5
5	M538R	0.1 ± 0.0	2.2 ± 0.3	95.5 ± 22.7	0.06	1.1 ± 0.0	20.5 ± 0.6	53.7×10^{-3}	58.5
6	S286N, Q377L	6.7 ± 0.2	4.0 ± 0.4	n.d.	1.67	(0.3 ± 0.0)	n.d.	30.6×10^{-3}	60.5
7	S286N, Q377V	5.8 ± 0.1	2.1 ± 0.2	n.d.	2.77	0.1 ± 0.0	12.7 ± 0.9	7.9×10^{-3}	58.5
8	S286T, Q377L	7.0 ± 0.1	2.1 ± 0.1	n.d.	3.50	(0.2 ± 0.0)	n.d.	19.9×10^{-3}	64.5
9	Q377M	5.0 ± 0.1	0.6 ± 0.1	n.d.	7.95	0.3 ± 0.0	28.7 ± 2	10.4×10^{-3}	62.0
10	S286E, Q377K	0.2 ± 0.0	0.9 ± 0.1	n.d.	0.22	(1.5 ± 0.0)	n.d.	153×10^{-3}	53.0
11	S286V, Q377T	0.9 ± 0.0	0.3 ± 0.0	141.7 ± 28.1	3.00	(3.4 ± 0.1)	n.d.	340×10^{-3}	65.5

[a] Turnover rate as a function of substrate concentration was presented in Figure S3 and S4. n.d. is not determined. Melting temperature (T_m) represented as the change of fluorescence signal over temperature is presented in Figure S5. All variants were purified to a comparable homogeneity (Figure S6)

[b] For variants 1, 2, 3, 6, 8, 10 and 11 substrate saturation was not achieved and kinetic constants could not be determined. Instead of k_{cat} values, the turnover rate at 100 mM aKG is given and k_{cat}/K_M was approximated by dividing the turnover rate at 100 mM aKG by this concentration.

[c] Activity profile of Var. 1 is identical to that of the wild type.

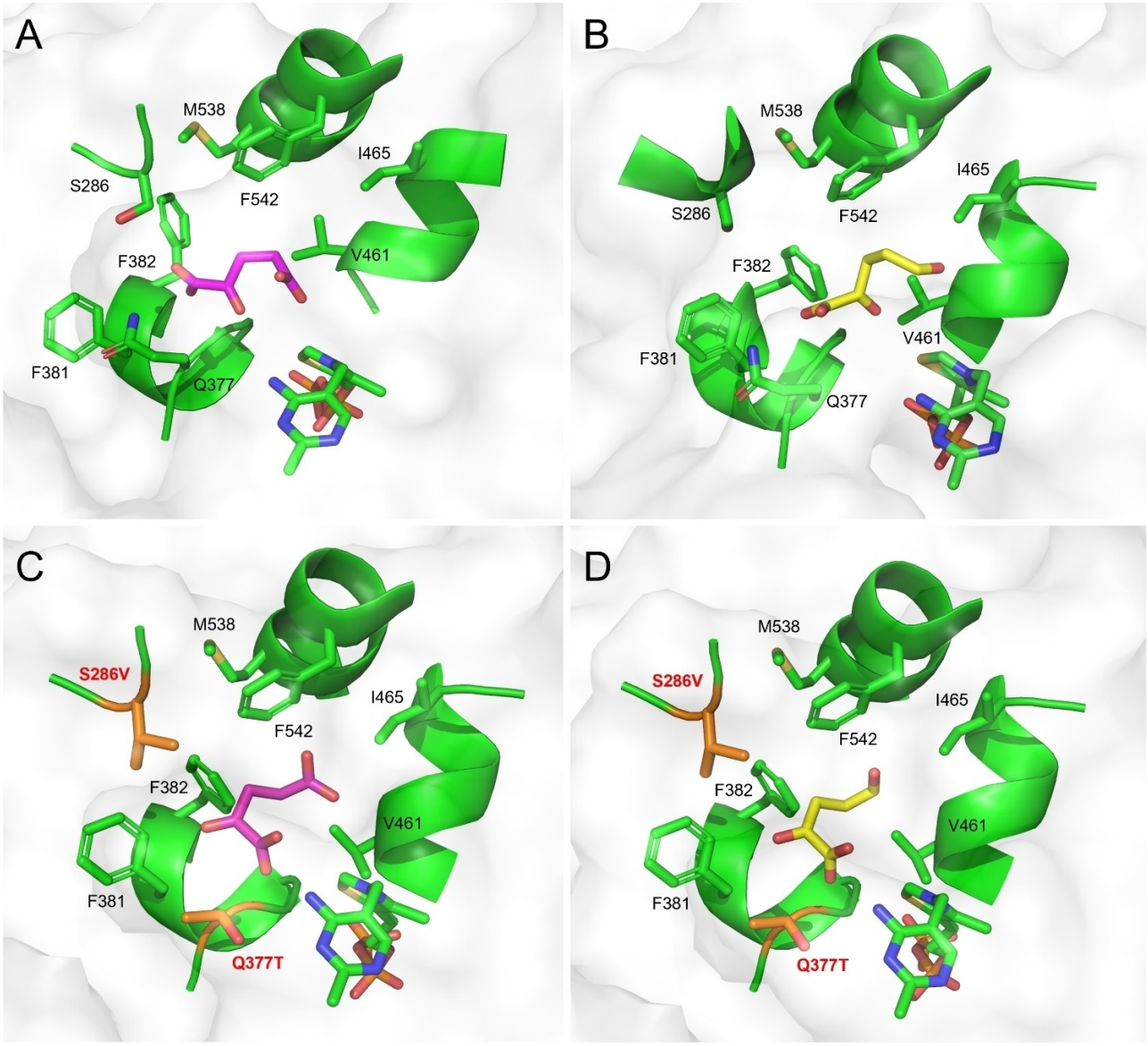

Figure 1. Docking result of KdcA with α-ketoglutarate (aKG, magenta; A) and α-ketoglutarate semialdehyde (KGSA, yellow; B) after pose refinement resulting from a 200 ns molecular dynamics simulation. Several amino acids shape the binding pocket of KdcA. Interactions with catalytic amino acids (28D, 112H, 113H) are not shown to ease visualization. The docked pose in the best performing variant, Var. 11 (S286V, Q377T) with aKG (C) and KGSA (D) are also shown. The substrates, cofactor, and binding site residues are shown in sticks representation, with the substituted residues highlighted in orange.

rational screening, we used the degenerate codon motif of NNS. We incorporated additional four mutations located on the surface as the starting template (Var. 1) based on the report from a previous study claiming these substitutions to enhance thermostability without compromising substrate specificity.[18] Indeed our activity assays confirmed the claim and showed that there was no significant difference in activity toward KGSA and aKG between the wild type enzyme and Var. 1 (data not shown).

Library Screening and Detailed Characterization of Engineered Variants

Prior to the screening campaign, we designed a universal pH-based assay to monitor enzyme activity by the concomitant change of pH upon decarboxylation. This approach was shown to be suitable for detecting activity of decarboxylase, transferase, and hydrolase.[19–21] In this work, we used bromothymol blue (BTB), which was shown to have high extinction coefficient and to be suitable in the range of pH 6 to 7. We embedded the assay in a liquid handling station to

increase the throughput and accuracy of the screening.[22] A more detailed description regarding the assay development is presented in the Supplementary Information and Figure S1.

From the first screening campaign targeting the substrate binding pocket of KdcA individually (Figure 1 A and B), we obtained a number of variants which appeared to show higher activities than the original template (Var. 1). After their mutations were confirmed by sequencing and subsequent purifications, the kinetic parameters of these variants were analyzed in more detail (Table 1). One variant having a substitution at position 286 from serine to threonine, S286T (Var. 2), showed a 50% increased k_{cat} for both substrates. Another variant carrying the Q377T substitution (Var. 3) showed a 4-fold increased catalytic efficiency (k_{cat}/K_M) toward KGSA and a 7-fold increased k_{cat} toward aKG. Molecular docking simulations of KGSA and aKG in Var. 3 showed that the substitution from glutamine to threonine creates space for KGSA and aKG, while keeping the ability to stabilize both substrates in the active site with the hydrogen bond between the hydroxyl group of threonine and the aldehyde or carboxylic group of KGSA and aKG, respectively (Figure S2). Interestingly, substitution to isoleucine at the same position (Var. 4) only showed beneficial effect toward KGSA (3.5-fold higher catalytic efficiency).

One last variant from the first screening campaign with M538R substitution (Var. 5) showed a modest increase in k_{cat} toward aKG but lost >30-fold in catalytic efficiency toward KGSA. The branching point for the two different products lies in KGSA, which for BDO production has to be decarboxylated and subsequently reduced and for succinic acid has to be oxidized first to aKG, which only then is decarboxylated. Accordingly, there are two decarboxylation reactions acting on similar substrates (aKG and KGSA), which have to be well balanced to allow parallel production of both products. Thus, Var. 5 that shows strong preference toward only one α-keto acid would not be suitable. It would, however, be suitable when succinic acid was the only desired product as it is no longer able to decarboxylate the intermediate KGSA efficiently in comparison to Var. 1.

From the first screening campaign, we concluded that position 286 and 377 are the most promising hotspots for improving activity toward KGSA and aKG. In the second screening campaign, we opted to saturate both positions simultaneously. We used combinations of sets of three primers to allow substitution to 19 amino acids excluding tryptophan, while still minimizing the number of variants screened.[23] The library was then generated via Gibson assembly and screened for activities toward KGSA and aKG. From the second screening campaign, we obtained four distinct variants that appeared to have increased activity toward KGSA (Var. 6 to 9) and two variants that appeared to have increased activity toward aKG (Var. 10 and 11). Catalytic properties of all variants are summarized in Table 1. The highest improvement of k_{cat} toward KGSA is registered by Var. 8 carrying double substitution, S286T, Q377 L. However, the K_M of Var. 8 is also slightly higher, giving an ample increase in catalytic efficiency of 1.6-fold. Furthermore, this variant also suffers from lower activity toward aKG in comparison to Var. 1. The improved k_{cat} toward KGSA observed for variants with substitution at position 377 could be rationalized partly by the loss of hydrogen-bonding with Q377, thus resulting in a faster product release. From the hits obtained from aKG screening, a variant with double substitution of S286 V, Q377T (Var. 11) showed an interesting kinetic behavior. Albeit the k_{cat} toward KGSA being decreased, its K_M is 4-fold lower in comparison to Var. 1, thus giving slightly higher overall catalytic efficiency. This variant further showed a 6-fold higher k_{cat} toward aKG in comparison to Var. 1.

All substitutions in the binding pocket changed the thermostability (measured as T_m in Table 1) of KdcA. To our surprise, substitution at position S286T (Var. 2) appeared to increase stability of KdcA considerably. This position was however not included in the previous study targeting stability of KdcA by stabilizing its catalytic center. It would be interesting to see if addition of S286T to the most stable variant reported earlier could further increase the stability without compromising activity toward the natural substrate, 2-ketoisovalerate.[18] Additionally, we were also interested in the activity obtained toward 2-keto-3-deoxy-D-xylonate (D-KDX) and 2-keto-3-deoxy-L-arabinonate (L-KDA), an α-keto acid intermediate of the Weimberg pathway from D-xylose and L-arabinose, respectively. In this work, it was of importance to have variants with minimal activity toward D-KDX as high activity toward D-KDX will compete with *Pp*D-KdpD, an auxiliary enzyme catalyzing dehydration of D-KDX to KGSA (Scheme 1).[14,24] Fortunately, all variants obtained did not exceed the activity of *Pp*D-KdpD (k_{cat}: 77 s^{-1}) toward D-KDX. The highest improvement toward D-KDX and L-KDA was recorded for Var. 3 (Figure 2). It is worth to note that decarboxylation of these two α-keto acids will result in a precursor of other valuable chiral compounds, namely (S)-BTO and (S)-HBL from D-KDX and (R)-BTO and (R)-HBL from L-KDA.[25,26]

Designing a Chemo-Enzymatic Approach for Co-production of BDO and Succinic Acid from D-xylose

Direct enzymatic production of BDO from D-xylose comprises one oxidation step followed by two reduction steps requiring one net equivalent of NADH. On the other hand, production of succinate from D-xylose

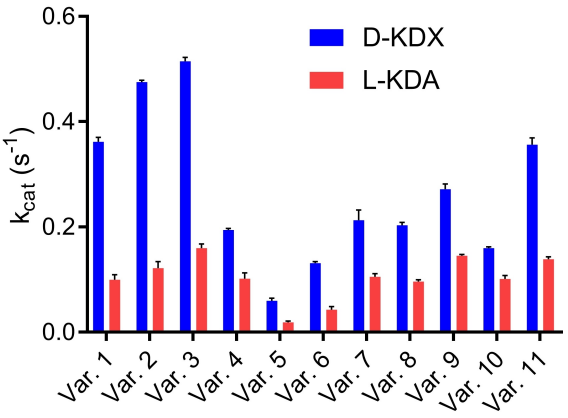

Figure 2. Activity of KdcA variants toward 2-keto-3-deoxy-D-xylonate (D-KDX) and 2-keto-3-deoxy-L-arabinonate (L-KDA). Activity was measured with 5 mM substrate in KPi 50 mM containing $MgCl_2$ 2.5 mM and ThDP 0.1 mM at 30 °C.

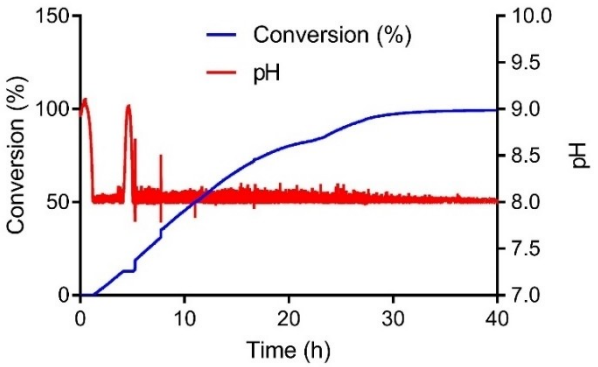

Figure 3. Oxidation of 40 mmol D-xylose to D-xylonate by 80 mg gold catalyst. Additional 40 mg gold catalyst was added after 23 h to push the reaction into completion. Conversion was estimated based on the amount of base (NaOH 2.5 M) titrated to the reaction solution.

via aKG produces three net equivalents of NADH from three oxidation steps. When both steps are combined a theoretical product ratio of 3:1 (BDO: succinic acid) will be obtained. In order to circumvent an imbalanced product ratio, the first oxidation can be performed by means of a cofactor-independent step. In this case, BDO production route will require two equivalents of NADH, while a succinic acid production route will yield two equivalents of NADH (Scheme 1). In previous studies, the proficiency and selectivity of gold catalysts toward oxidation of a wide range of aldose sugars have been demonstrated.[27]

One of the major drawbacks in the use of metal catalyst in biocatalytic reaction is the incompatibility of the two catalysts in one-pot. The catalyst is disturbed in the presence of protein, thus requiring a large amount of catalyst used. On the other hand, biocatalysts may not be stable in the reaction condition where the chemical reaction is performed.[28,29] Additionally, oxidation by gold catalyst requires constant bubbling of oxygen, which is not always directly amenable to enzymatic processes.[30,31] Thus to harness the potential of both systems, we opted for a one-pot multi-step synthesis approach. In this way, D-xylose was first oxidized by the gold catalyst at suitable condition (50 °C, pH 8). Subsequently, an enzymatic biotransformation of D-xylonate to BDO and succinic acid was performed at 30 °C and pH 7. No intermediate purification was necessary in this approach.

Oxidation of D-xylose was then carried out in an automatic titration unit to maintain the pH at 8. This step was successfully performed with 40 mmol initial D-xylose in a volume of 40 ml. Addition of gold catalyst was necessary to push the reaction into completion. After 40 h oxidation, >98% conversion was achieved and final concentration of D-xylonate reached 1 M (Figure 3). After removal of the catalyst by means of centrifugation, the final concentration of D-xylonate was adjusted to 100 mM and the reaction pH to 7. A combination of enzyme cocktails and cofactors were added to the solution and enzymatic biotransformation was started. Three different variants of KdcA were tested while maintaining the other enzymes constant.

In the enzymatic biotransformation step, D-xylonate would undergo two dehydration steps to yield KGSA. As shown in a previous study, KGSA is not a stable intermediate; thus, its presence needs to be minimized.[24] As two dehydration steps are cofactor-independent, the concentration of KGSA was regulated by the activity of the two dehydratases (*Pu*DHT and *Pp*D-KdpD) added in the system. An aldehyde dehydrogenase from *Pseudomonas putida* (*Pp*KgsaDH) was used to oxidize KGSA to aKG in previous studies.[20,38] We tested this enzyme toward oxidation of succinic semialdehyde (SSA), the decarboxylation product of aKG, to yield succinic acid. Unfortunately, *Pp*KgsaDH did not show any significant activity. To minimize the total number of enzymes used, we opted to find a promiscuous aldehyde dehydrogenase. After screening our oxidoreductase library, we found a promiscuous aldehyde dehydrogenase from *E. coli* (*Ec*SAD), which can oxidize both aldehydes (KGSA and SSA) efficiently.[39] In parallel, KGSA was also subjected to decarboxylation to yield succinaldehyde (SA) prior to undergoing double reduction to yield BDO. *Ec*AdhP has been shown as a suitable catalyst for the reduction step.[20]

After finding all suitable auxiliary enzymes, the enzymatic biotransformation was then followed for 24 h. All KdcA variants were able to achieve >90% theoretical yield of BDO and succinic acid at the end of the biotransformation (Figure 4). To our surprise, Var. 3 with significantly higher activities toward both

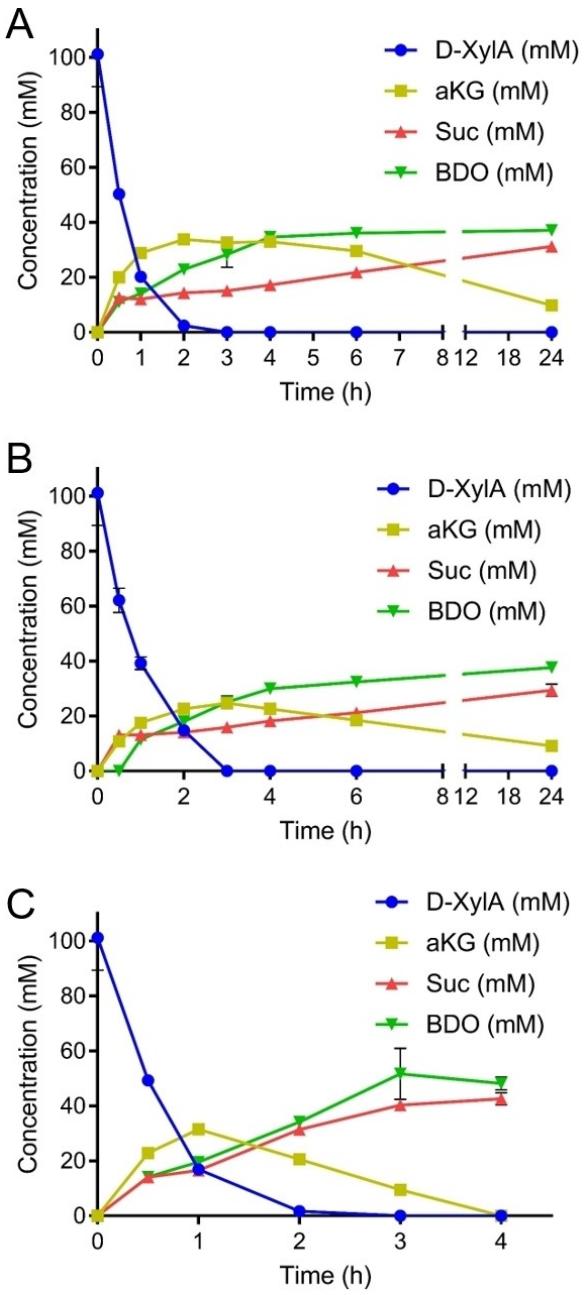

Figure 4. In vitro transformation of D-xylonate (D-XylA) to 1,4-butanediol (BDO) and succinic acid (Suc) via α-ketoglutarate (aKG) catalyzed by Var. 1 (A), Var. 3 (B), Var. 11 (C). Exemplary chromatogram profiles are presented in Figure S7 and S8.

substrates performed in a similar manner as Var. 1 that showed barely activity toward aKG. In contrast, the best performance was registered when Var. 11 was used, reaching >95% theoretical yield just after 4 h. No aKG was observed when Var. 11 was used, unlike Var. 1 and 3 that still recorded up to 10% aKG even after 24 h biotransformation.

The rather unexpected high yield when Var. 1 was used could be due to side reactivity of *Ec*SAD. In this case, succinic acid was formed from double oxidation of succinaldehyde, instead of from intended oxidation of succinic semialdehyde. Due to unavailability of commercial succinaldehyde, we were unable to confirm this activity. However, *Ec*SAD demonstrated activity toward glutaraldehyde (data not shown) giving a strong suggestion on the side reactivity toward succinaldehyde. The fact that Var. 11 outperformed Var. 3 was likely due to its rather comparable activities toward KGSA and aKG at lower concentrations. For example, at 5 mM substrates concentration, Var. 11 showed a k_{cat} of 0.7 s^{-1} toward KGSA and 0.5 s^{-1} toward aKG. Conversely, at 5 mM substrates concentrations, Var. 3 showed a significantly higher k_{cat} toward KGSA as compared with aKG (3.5 s^{-1} against 0.5 s^{-1}) (Figure S4). These results may suggest, when a promiscuous enzyme catalyzing two or more reactions simultaneously in a cascade reaction is applied, it is more beneficial to use an enzyme variant, which shows a similar degree of catalytic efficiency for all the substrates. Similar observation was also reported when *in vivo* system was used.[32]

Conclusion

Polybutylene succinate (PBS) is an emerging bioplastic, which is assembled from polymerization of 1,4-butanediol and succinic acid. With its melting point above 100 °C, PBS is categorized as thermoplastic and has found applications ranging from mulching film to biomedical devices.[11,12] Albeit PBS is categorized as bioplastic, the two monomeric constituents of PBS are still largely manufactured from petrochemicals, in particular 1,4-butanediol; thus, depreciating the "bio" label of PBS. As one of the major components of hemicellulose, D-xylose is of great interest to be utilized as a source of second-generation chemical production. Direct transformation of D-xylose to BDO has been demonstrated in previous studies.[14,15] However, no studies reported on the use of D-xylose for succinic acid production. One of the key steps for the production of succinic acid is decarboxylation of α-ketoglutarate. In this work, we used *in silico* docking studies with semi rational designs to engineer a promiscuous branched chain α-keto acid decarboxylase (KdcA). After developing a suitable screening assay embedded in a liquid handling station, we screened <2000 variants to find a number of variants with improved activity toward aKG and KGSA (the intermediate for BDO production). Direct enzymatic biotransformation of D-xylose to 1,4-butanediol and succinic acid will result in a 3:1 product ratio due to imbalance redox requirement. To circumvent this undesired product ratio, the first oxidation was performed chemically using a gold catalyst. As the

gold catalyst is incompatible to be applied directly with enzymatic approach, we designed a one-pot multi-steps strategy. With this approach we were able to transform D-xylose to 1,4-butanediol and succinic acid (1:1). The utilization of an improved KdcA variant in the enzymatic step was proven to increase productivity and final yield of 1,4-butanediol and succinic acid in comparison when the original KdcA variant was used. This study underlines the benefit of applying an integrative approach, namely protein engineering and chemical oxidation, toward the realization of second-generation chemical production.[33]

Experimental Section

Molecular Docking and Molecular Dynamics

The protein structures of KdcA (PDB-ID: 2vbg) were used for the *in silico* calculations. An AlphaFold structure was prepared for KdcA and superposed with the crystal structure 2vbg.[17] The missing loops at position 182–187 and 342–344 were replaced by the loop conformations predicted by AlphaFold. For the molecular docking and molecular dynamics simulations, the refined model was prepared with the YASARA modelling suite, followed by an energy minimization using the YASARA engine. The protonation states of all residues were predicted by PDB2PQR at pH = 6.5.[34] Based on a visual check, the protonation of the following binding site residues were deprotonated: E49, E376, and D429, while D26, H112, and E462 were protonated to retain the respective hydrogen bond network. The substrates were built in YASARA, and the ThDP (thiamine diphosphate) cofactor was protonated manually. Molecular docking simulations were performed with AutoDock VINA.[35] A cubic simulation box of 22.5 Å in each dimension was placed around the binding site with a spacing of 0.375 Å. For subsequent molecular dynamics simulations, AMBER ff14SB force field parameters were defined for the protein, and GAFF for the ThDP cofactor and substrates.[36,37] AM1-BCC charges were derived using antechamber. The system was solvated in a rectangular box consisting of TIP3P water applying a buffer region of 12 Å around the protein, and counter ions were added to neutralize the system.[38] The energy minimization and heat up procedure, as well as the simulation setup procedure was performed as described in a previous study.[39] The molecular dynamics simulations were performed with the pmemd.CUDA MD engine from AMBER18.[40] After 200 ns simulation time, a hierarchical cluster analysis with epsilon of 1.5 was performed on all frames with cpptraj from the Amber18/AmberTools18 software package. The representative frame of the largest cluster was considered as the equilibrated docked pose.

Enzyme Kinetic Characterization

Activity of KdcA variants were determined by coupled assays. In brief, the product of decarboxylation, aldehyde was reacted with appropriate alcohol dehydrogenase in the presence of NADH or aldehyde dehydrogenase in the presence of NAD^+. The consumption or formation of NADH was monitored at 340 nm. Activity toward KGSA was measured by coupling with *Ec*AdhP in the presence of NADH. Activity toward aKG was measured by coupling with *Ec*SAD in the presence of NAD^+. Activity toward KDX and KDA were monitored by coupling with *Ec*YgjB (LND) and NADH. All reaction solutions contained 50 mM KPi pH 7.0, 0.1 mM ThDP, 2.5 mM $MgCl_2$, 0.5 mM NADH or NAD^+, 10 U/ml coupling enzyme. The activity measurement was conducted in 96 MTP at 30 °C. Turnover number (k_{cat}) is defined as the number of NADH molecule consumed or produced per molecule of KdcA per second.

Oxidation of D-xylose with Gold Catalyst

In brief, 40 mmol of D-xylose was dissolved in 30 ml water. After all D-xylose powder was completely dissolved, final volume was adjusted to 40 ml with water. The solution was transferred to an automatic titratror (Metrohm, Germany). The solution was bubbled with O_2 at 40 ml/min and stirred rigorously. Subsequently, 80 mg gold catalyst 0.5% (Evonik, Germany) was added to the solution. The titration was shortly started with 2.5 M NaOH used as the base. The reaction was monitored by following the amount of NaOH added to the reaction solution. The reaction progressed linearly and appeared to stall after 23 h. Another 40 mg gold catalyst was added to restart the reaction. After 40 h, >98% theoretical conversion was achieved. The reaction was then stopped, and the gold catalyst was removed by means of centrifugation. Subsequently, D-xylonate was quantified by HPLC coupled to a UV-detector at 210 nm. Metrosep A Supp 16–250 (Metrohm, Germany) was used as the stationary phase and ammonium bicarbonate buffers as the mobile phase. The solution was directly used for the subsequent enzymatic reaction. The remaining solution was stored at 4 °C and stable for several weeks.

Biotransformation of D-xylonate

For enzymatic transformation of D-xylonate to 1,4-butanediol (BDO) and succinic acid, enzyme cocktail was added to D-xylonate that was produced from the previous step. The final reaction solution contained 100 mM D-xylonate, 0.1 mM ThDP, 2.5 mM $MgCl_2$, 1 mM NAD^+, 2 U/ml *Pu*DHT, 1 U/ml *Pp*D-KdpD, 4 U/ml *Ec*AdhP, 4 U/ml *Ec*SAD. Different variants of KdcA tested were normalized to the final concentration of 1 mg/ml. The reaction was performed at 30 °C, 500 rpm (orbital shaker). No buffer was added other than the one already presents in the enzyme solution. Samples were withdrawn every certain time to monitor the progress of the reaction. The sample was diluted 1:1 with 5 mM H_2SO_4 and filtered through 10 KDa centrifugal column to stop the reaction. The filtrate was then analyzed using an ion-exclusion column (RezexROA-Organic Acid H+(8%), Phenomenex, Germany) connected to an HPLC with a UV detector 210 nm and run isocratically using H_2SO_4 2.5 mM at 70 °C for 30 min.

Production of KGSA

D-Xylonate 0.5 M, 10 ml from the chemical oxidation step was reacted with *Pu*DHT (1 U/ml) to produce 2-keto-3-deoxy-D-xylonate (KDX). $MgCl_2$ 1 mM (end concentration) was added. The reaction was performed in a 50 ml non-baffled Erlenmeyer

flask, at 30 °C, 150 rpm overnight. The following day, after the completion of the first dehydration step was confirmed by HPLC, *Pp*D-KdpD (2 U/ml) was added to the reaction solution to convert D-KDX to 2-ketoglutaralsemialdehyde (KGSA). The reaction was followed overtime by HPLC. After all KDX was converted to KGSA (approximately 5 h), the reaction solution was directly filtered through a 10 KDa centrifugal column (Sartorius, Germany). The solution was frozen at −20 °C. The reaction was assumed to go into completion where there was no more substrate detected by HPLC (detection limit 0.05 mM). The final concentration of KDX and KGSA were estimated to reach >95% for every dehydration step.

Acknowledgements

The authors wished to thank Samed Güner and Torben Hüsing for fruitful discussion. The authors would like to acknowledge partial funding from German Federal Ministry for Education and Research through HotSysAPP (Grant No. 031L0078F) and BINOM (Grant No. 031B1055). Open Access funding enabled and organized by Projekt DEAL.

References

[1] V. Narisetty, R. Cox, R. Bommareddy, D. Agrawal, E. Ahmad, K. K. Pant, A. K. Chandel, S. K. Bhatia, D. Kumar, P. Binod, V. K. Gupta, V. Kumar, *Sustain. Energy Fuels* **2022**, *6*, 29–65.
[2] Z. Zhao, M. Xian, M. Liu, G. Zhao, *Biotechnol. Biofuels* **2020**, *13*, DOI 10.1186/s13068-020-1662-x.
[3] J. S. Van Dyk, B. I. Pletschke, *Biotechnol. Adv.* **2012**, *30*, 1458–1480.
[4] K. N. G. Valdehuesa, K. R. M. Ramos, G. M. Nisola, A. B. Bañares, R. B. Cabulong, W. K. Lee, H. Liu, W. J. Chung, *Appl. Microbiol. Biotechnol.* **2018**, *102*, 7703–7716.
[5] M. K. McClintock, J. Wang, K. Zhang, *Front. Microbiol.* **2017**, *8*, DOI 10.3389/fmicb.2017.02310.
[6] M. de la Plaza, P. Fernández de Palencia, C. Peláez, T. Requena, *FEMS Microbiol. Lett.* **2004**, *238*, 367–374.
[7] B. A. Smit, J. E. T. Van Hylckama Vlieg, W. J. M. Engels, L. Meijer, J. T. M. Wouters, G. Smit, *Appl. Environ. Microbiol.* **2005**, *71*, 303–311.
[8] R. Miao, H. Xie, F. M. Ho, P. Lindblad, *Metab. Eng.* **2018**, *47*, 42–48.
[9] W. S. Mak, S. Tran, R. Marcheschi, S. Bertolani, J. Thompson, D. Baker, J. C. Liao, J. B. Siegel, *Nat. Commun.* **2015**, *6*, DOI 10.1038/ncomms10005.
[10] J. Tian, R. Bryk, M. Itoh, M. Suematsu, C. Nathan, *Proc. Nat. Acad. Sci.* **2005**, *102*, 10670–10675.
[11] M. Puchalski, G. Szparaga, T. Biela, A. Gutowska, S. Sztajnowski, I. Krucińska, *Polymers (Basel).* **2018**, *10*, 1–12.
[12] L. Aliotta, M. Seggiani, A. Lazzeri, V. Gigante, P. Cinelli, *Polymers (Basel).* **2022**, *14*, 1–23.
[13] "Bioplastics market data," can be found under https://www.european-bioplastics.org/market/, **2021**.
[14] S. Sutiono, A. Pick, V. Sieber, *Green Chem.* **2021**, *23*, 3656–3663.
[15] Y. S. Tai, M. Xiong, P. Jambunathan, J. Wang, J. Wang, C. Stapleton, K. Zhang, *Nat. Chem. Biol.* **2016**, *12*, 247–253.
[16] C. L. Berthold, D. Gocke, M. D. Wood, F. J. Leeper, M. Pohl, G. Schneider, *Acta Crystallogr. Sect. D* **2007**, *63*, 1217–1224.
[17] J. Jumper, R. Evans, A. Pritzel, T. Green, M. Figurnov, O. Ronneberger, K. Tunyasuvunakool, R. Bates, A. Žídek, A. Potapenko, A. Bridgland, C. Meyer, S. A. A. Kohl, A. J. Ballard, A. Cowie, B. Romera-Paredes, S. Nikolov, R. Jain, J. Adler, T. Back, S. Petersen, D. Reiman, E. Clancy, M. Zielinski, M. Steinegger, M. Pacholska, T. Berghammer, S. Bodenstein, D. Silver, O. Vinyals, A. W. Senior, K. Kavukcuoglu, P. Kohli, D. Hassabis, *Nature* **2021**, *596*, 583–589.
[18] S. Sutiono, J. Carsten, V. Sieber, *ChemSusChem* **2018**, *11*, 3335–3344.
[19] K. Yu, S. Hu, J. Huang, L.-H. Mei, *Enzyme Microb. Technol.* **2011**, *49*, 272–276.
[20] D. Yi, T. Devamani, J. Abdoul-Zabar, F. Charmantray, V. Helaine, L. Hecquet, W. D. Fessner, *ChemBioChem* **2012**, *13*, 2290–2300.
[21] L. E. Janes, A. C. Löwendahl, R. J. Kazlauskas, *Chem. A Eur. J.* **1998**, *4*, 2324–2331.
[22] A. Pick, B. Beer, R. Hemmi, R. Momma, J. Schmid, K. Miyamoto, V. Sieber, *BMC Biotechnol.* **2016**, *16*, DOI 10.1186/s12896-016-0308-3.
[23] L. Tang, H. Gao, X. Zhu, X. Wang, M. Zhou, R. Jiang, *BioTechniques* **2012**, *52*, 149–158.
[24] S. Sutiono, B. Siebers, V. Sieber, *Appl. Microbiol. Biotechnol.* **2020**, *104*, 7023–7035.
[25] J. Wang, X. Shen, R. Jain, J. Wang, Q. Yuan, Y. Yan, *Metab. Eng.* **2017**, *41*, 39–45.
[26] S. Sutiono, I. Zachos, L. Paschalidis, A. Pick, J. Burger, V. Sieber, *ACS Sustainable Chem. Eng.* **2023**, *11*, 6592–6599.
[27] J. M. Sperl, J. M. Carsten, J.-K. Guterl, P. Lommes, V. Sieber, *ACS Catal.* **2016**, *6*, 6329–6334.
[28] M. A. S. Mertens, F. Thomas, M. Nöth, J. Moegling, I. El-Awaad, D. F. Sauer, G. V. Dhoke, W. Xu, A. Pich, S. Herres-Pawlis, U. Schwaneberg, *Eur. J. Org. Chem.* **2019**, *2019*, 6341–6346.
[29] S. Mathew, A. Sagadevan, D. Renn, M. Rueping, *ACS Catal.* **2021**, *11*, 12565–12569.
[30] M. Dias Gomes, B. R. Bommarius, S. R. Anderson, B. D. Feske, J. M. Woodley, A. S. Bommarius, *Adv. Synth. Catal.* **2019**, *361*, 2574–2581.
[31] B. Beer, A. Pick, V. Sieber, *Metab. Eng.* **2017**, *40*, 5–13.
[32] G. S. Chen, S. W. Siao, C. R. Shen, *Sci. Rep.* **2017**, *7*, 11284.
[33] J. M. Woodley, *Philos. Trans. R. Soc. London* **2018**, *376*, DOI 10.1098/rsta.2017.0062.
[34] E. Jurrus, D. Engel, K. Star, K. Monson, J. Brandi, L. E. Felberg, D. H. Brookes, L. Wilson, J. Chen, K. Liles, M. Chun, P. Li, D. W. Gohara, T. Dolinsky, R. Konecny, D. R. Koes, J. E. Nielsen, T. Head-Gordon, W. Geng, R.

Krasny, G.-W. Wei, M. J. Holst, J. A. McCammon, N. A. Baker, *Protein Sci.* **2018**, *27*, 112–128.
[35] O. Trott, A. J. Olson, *J. Comput. Chem.* **2010**, *31*, 455–461.
[36] J. Wang, R. M. Wolf, J. W. Caldwell, P. A. Kollman, D. A. Case, *J. Comput. Chem.* **2004**, *25*, 1157–1174.
[37] J. A. Maier, C. Martinez, K. Kasavajhala, L. Wickstrom, K. E. Hauser, C. Simmerling, *J. Chem. Theory Comput.* **2015**, *11*, 3696–3713.
[38] W. L. Jorgensen, J. Chandrasekhar, J. D. Madura, R. W. Impey, M. L. Klein, *J. Chem. Phys.* **1983**, *79*, 926–935.
[39] O. Melse, S. Sutiono, M. Haslbeck, G. Schenk, I. Antes, V. Sieber, *ChemBioChem* **2022**, *23*, e202200088.
[40] D. A. Case, I. Y. Ben-Shalom, S. R. Brozell, D. S. Cerutti, T. E. Cheatham III, V. W. D. Cruzeiro, T. A. Darden, R. E. Duke, D. Ghoreishi, M. K. Gilson, H. Gohlke, A. W. Goetz, D. Greene, R. Harris, N. Homeyer, Y. Huang, S. Izadi, A. Kovalenko, T. Kurtzman, T. S. Lee, S. Le Grand, P. Li, C. Lin, J. Liu, T. Luchko, R. Luo, D. J. Mermelstein, K. M. Merz, Y. Miao, G. Monard, C. Nguyen, H. Nguyen, I. Omelyan, A. Onufriev, F. Pan, R. Qi, D. R. Roe, A. Roitberg, C. Sagui, S. Schott-Verdugo, J. Shen, C. L. Simmerling, J. Smith, R. Salomon Ferrer, J. Swails, R. C. Walker, J. Wang, H.Wei, R. M. Wolf, X. Wu, L. Xiao, D. M. Yorkand, P. A. Kollman, *AMBER 2018*, University Of California, San Francisco, **2018**.